Published in final edited form as:
Neurosci Res. 2011 November ; 71(3): 226–234. doi:10.1016/j.neures.2011.07.1832.

Expression of Connexin 57 in the Olfactory Epithelium and Olfactory Bulb

Chunbo Zhang
Department of Biological and Chemical Sciences, Illinois Institute of Technology, Chicago, IL 60616, USA

Abstract

In the visual system, deletion of connexin 57 (Cx57) reduces gap junction coupling among horizontal cells and results in smaller receptive fields. To explore potential functions of Cx57 in olfaction, *in situ* hybridization and immunohistochemistry methods were used to investigate expression of Cx57 in the olfactory epithelium and olfactory bulb. Hybridization signal was stronger in the olfactory epithelial layer compared to the connective tissue underneath. Within the sensory epithelial layer, hybridization signal was visible in sublayers containing cell bodies of basal cells and olfactory neurons but not evident at the apical sublayer comprising cell bodies of sustentacular cells. These Cx57 positive cells were clustered into small groups to form different patterns in the olfactory epithelium. However, individual patterns did not associate with specific regions of olfactory turbinates or specific olfactory receptor zones. Patched distribution of hybridization positive cells was also observed in the olfactory bulb and accessory olfactory bulb in layers where granule cells, mitral cells, and juxtaglomerular cells reside. Immunostaining was observed in the cell types described above but the intensity was weaker than that in the retina. This study has provided anatomical basis for future studies on the function of Cx57 in the olfactory system.

Keywords

connexin; gap junction; olfactory system; gene expression; neuron; murine

1. Introduction

In light of genetic, molecular and functional studies on gap junctions and gap junction protein subunits, connexins, it has been demonstrated that this gene family is involved in a broad range of biological and physiological processes. Among twenty connexin (Cx) genes discovered in mouse and twenty-one in human genomes, nearly half of them are expressed in the nervous system. While ultrastructural studies demonstrate that Cx36 and Cx45 are expressed in neurons (Rash et al., 2001; Pereda et al., 2003; Rash et al., 2005), molecular biological and transgenic studies indicate that Cx43 and Cx57 are also expressed in neurons (Zhang et al., 2000; Hombach et al., 2004) and have significant physiological functions (Zhang and Restrepo, 2005; Shelley et al., 2006; Zhang, 2010). A recent study has shown

Corresponding Address: Chunbo Zhang, Department of Biological and Chemical Sciences, Illinois Institute of Technology. 3101 S. Dearborn Street, LS182, Chicago, IL 60616, USA, Tel: 1-312-567-3575, Fax: 1-312-567-3494, ZhangC@iit.edu.

that Cx30.2 is another neuronal gap junction protein although its function remains undefined (Kreuzberg et al., 2008).

Presence of gap junctions in the olfactory system has been observed at various levels. In early studies, freeze fracture data showed the presence of gap junctions in the olfactory bulb in granule cells (Reyher et al., 1991), and in mitral and tufted cells (Miragall et al., 1996). A few recent elegant ultrastructural studies have demonstrated that gap junctions are found in neuronal processes of periglomerular cells, mitral cells and tufted cells (Kosaka and Kosaka, 2003, 2004, 2005). It was later shown that some of these gap junctions are formed by Cx36 or Cx45 (Kosaka et al., 2005; Rash et al., 2005), and that Cx36 gap junctions are responsible for coordination among mitral cells (Christie et al., 2005). Using *in situ* hybridization and immunohistochemistry methods, we have demonstrated that Cx36, Cx43 and Cx45 are expressed in neurons in the olfactory bulb including periglomerular cells, tufted cells, mitral cells and granule cells (Zhang et al., 2000; Zhang and Restrepo, 2002, 2003).

Gap junction plaques are found in the olfactory epithelium by freeze fracture techniques (Koling et al., 1988; Rash et al., 2005). An immunohistochemical study showed that Cx43 was expressed in sustentacular cells of the olfactory epithelium, in fibroblasts in the underlying connective tissue, and in ensheathing cells within axon bundles (Miragall et al., 1992). Using *in situ* hybridization, immunohistochemistry, mouse genetics and olfactory bulb ablation approaches we have demonstrated that Cx43 is expressed in mature and immature olfactory neurons in addition to the aforementioned cells (Zhang et al., 2000). We have further shown that Cx36 and Cx45 are expressed in olfactory neurons and neurons in the olfactory bulb (Zhang and Restrepo, 2002, 2003). Expression of Cx36, Cx43 and Cx45 in the olfactory epithelium and olfactory bulb exhibits distinct spatial distribution patterns. In this study, I provide evidence on expression of Cx57 in olfactory neurons and basal cells in the olfactory epithelium and in neurons of the olfactory bulb.

2. Materials and methods

2.1. Animals and tissue preparation

Adult male C57BL/6 mice from the Jackson Laboratory (Bar Harbor, ME) were used in the study. Mice, 3–6 months of age, were anesthetized and perfused transcardially with phosphate-buffered saline (PBS, pH 7.4) followed by perfusion with ice cold 4% paraformaldehyde in PBS. The whole nasal turbinates and olfactory bulb were dissected out and fixed in 4% paraformaldehyde overnight. For cryoprotection, 25% sucrose was added in the fixation solution. The nasal turbinates together with the olfactory bulb were then embedded in Tissue-Tek O.C.T. compound (Sakura Finetek), and tissue sections (12 μm) were cut on a cryostat at −18°C and stored at −80°C. Every tenth section, from the anterior of the turbinates to the end of the olfactory bulb, was processed and examined. All procedures were performed under protocols approved by the Illinois Institute of Technology Animal Care and Use Committee.

2.2. Real time PCR and reverse transcription PCR

To determine whether the olfactory epithelium expresses Cx57, reverse transcription PCR (RT-PCR) and real time PCR were used to detect the Cx57 transcript. Total RNA was extracted from mouse turbinates with TRIzol reagent according to the manufacturer's direction (Invitrogen). Total RNA was then treated with RQ1 RNase-free DNase (Promega) to eliminate possible genomic DNA contamination before being used for real time PCR and RT-PCR. Absence of genomic DNA contamination was confirmed by PCR reaction using a pair of primers amplifying a fragment of intron spanning actin (Primer-Actin): ATGAAGATCCTGACCGAGCG and TACTTGCGCTCAGGAGGAGC. A single band

approximately 433 bp was obtained, indicating amplification from cDNA. Samples contaminated with genomic DNA would have led to a second band at 663 bp.

For RT-PCR of Cx57, reverse transcriptase III from Invitrogen was used according to the manufacturer's direction. Two microliters of cDNA were PCR amplified with the primer pair A: AGAAAATTGAGAGCTGTGCA and AGAGACCGTGAGCTTCCTGA (Primer-Cx57A). This resulted in a 388 bp DNA fragment near C-terminus of the Cx57 coding region having no homology to other known murine connexins according to a BLAST search (from 971-1339 based on NM_010289.2). One-step real time quantitative PCR was conducted in Research Technology Support Facility at Michigan State University with the primer pair B (Primer-Cx57B): GAAGTCGCAAGGCCAGCTT and CACTATGCCGTTGTCCCTTTTC. Reactions were carried out on an ABI 7700 real time PCR thermalcycler (Applied Biosystems) under the following conditions: 48°C for 30 min, 95°C for 10 min, and 40 cycles of 95°C for 15 s followed by 60°C for 1 min.

2.3. RNA probe preparation and in situ hybridization

The experimental strategies used here were similar to what was described previously (Zhang et al., 2000). Since the 388 bp Cx57 cDNA fragment described above has no homology to other known murine connexins, this cDNA fragment was cloned into pCRII (Invitrogen), sequenced and used as templates for the synthesis of Cx57 cRNA probes.

Digoxigenin labeled sense and antisense cRNA probes were used for *in situ* hybridization. Coronal sections of whole turbinates and the olfactory bulb sampled every 120 μm apart were hybridized with antisense cRNA and their adjacent sections hybridized with sense cRNA as the control. Tissue sections were rinsed three times for 10 min each in PBS before a 2-hr incubation in prehybridization solution (50% deionized formamide, 1x Denhart's solution, 750 mM sodium chloride, 25 mM ethylenediamine-tetraacetic acid (EDTA), 25 mM piperazine-N,N'-bis[2-ethane-sulfonic acid] (PIPES), pH 7.0, 0.25 mg/ml salmon sperm DNA, 0.25 mg/ml poly A acid and 0.2% SDS). Sections were then hybridized with the same amount of sense (as the control) or antisense digoxigenin-labeled cRNA probes in the hybridization solution (prehybridization solution containing 2.5% dextran sulfate) at 60°C for 16–20 hrs. After hybridization, sections were washed three times for a total of 60 min in 2xSSC/0.3% Tween-20 followed by three washes for a total of 60 min in 0.2xSSC/ 0.3% Tween-20 at 65°C.

For the detection of digoxigenin-labeled probes, the sections were treated for 2 hrs in blocking solution (10% sheep serum/2% bovine albumin/0.3% Tween-20). The sections were then incubated overnight (16–20 hrs) at 4°C with alkaline phosphatase-conjugated anti-digoxigenin Fab fragments (1:1000 in blocking solution, Roche). Unbound Fab fragments were washed away and the sections were incubated in nitroblue tetrazolium chloride and 5-bromo-4-chloro-3-indolyl phosphate substrate (NBT/BCIP, Roche) until the staining was developed (in 5 hrs). Color reactions were terminated at the same time period for all slides including the controls. The control slides, hybridized with the sense Cx57 cRNA probe, were conducted identically as the experimental slides. Five mice were used for *in situ* hybridization.

2. 4. Immunohistochemistry

Two antibodies against Cx57 are available from Invitrogen: Ab40-4800CT was raised in rabbits against amino acid 434–446 of murine Cx57, and Ab40-5000MID raised in rabbit against amino acid 248–263 of murine Cx57. Antibodies were tested for specificity by Western blot analysis of protein homogenates of mouse olfactory turbinates. The Ab40-4800CT revealed a very weak band with the molecular weight corresponding to Cx57

and a few strong bands in other locations, a pattern similar to a published result using retinal homogenates (Ciolofan et al., 2007). This antibody was not used further since a majority of immunoreactivity was irrelevant to Cx57. The Ab40-5000MID specifically recognizes a single band at the corresponding position in Western analysis (Fig. 1A). Thus, only Ab40-5000MID was used here for immunohistochemistry.

Immunohistochemistry was conducted to the olfactory epithelium and olfactory bulb of adult mouse. Before immunohistochemistry, an antigen retrieval method was used to facilitate antigen-antibody recognition. Slides were incubated in 0.01M sodium citrate buffer (pH 6.0) at 60°C for 30 min before regular immunohistochemistry. The Ab40-5000MID antibody against Cx57 was visualized by indirect immunofluorescence with a secondary antibody linked to Alexa Fluor 488 (Invitrogen). Adjacent tissue sections were preceded in parallel as the negative control by the omission of the primary antibody. Slides were treated with Sudan black to block autofluorescences (Baschong et al., 2001; Viegas et al., 2007). A confocal laser-scanning microscope (Zeiss LSM 510) was used to examine immunofluorescence.

2.5. Photomicrographs and image processing

Except for images acquired with confocal microscopy, bright field photomicrographs were obtained with a Spot RT cooled CCD camera from Diagnostic Imaging using the software provided by the manufacturer. The camera was mounted on a Nikon epifluorescence (TE 2000-U) research microscope. All images were then transferred to Adobe Photoshop for presentation. Comparative images were processed identically if changes in contrast were made.

For quantitative analysis of hybridization signal, the comparative images were photographed under the same exposure condition and the images were analyzed using the NIH ImageJ software (http://rsbweb.nih.gov/ij/). The ImageJ program reports averaged grayscales ranging from 0.000 to 255.000 in a selected area where 255.000 represents white in the area. In the analysis, a low grayscale was associated with the area where the hybridization signal was intensive while the background signal had a larger grayscale. The Relative Hybridization Intensity (RHI) used in the text represents the grayscale of background subtracted from the grayscale of examining area, which means that a larger number of RHI indicates stronger hybridization signal in the area. Data values were presented in terms of mean and the standard error of the mean.

3. Results

3.1. Expression of connexin 57 transcripts

To determine whether Cx57 is expressed in the olfactory epithelium, RT-PCR and real time PCR methods were used. Total RNA was extracted from mouse nasal turbinates and treated with RQ1 RNase-free DNase (Promega, WI) to eliminate genomic DNA contamination. RT-PCR and real-time PCR were conducted as described above. PCR amplification of cDNA of nasal turbinates using the primer pair Primer-Cx57A revealed a single band of the expected size (Fig. 1B). Real time PCR analysis using Primer-Cx57B showed a linear decrease of the threshold cycles when the amount of total RNA was increased logarithmically (Fig. 1C). These results indicate that Cx57 is expressed in the olfactory epithelium.

To investigate cell specificity and distributions of Cx57 expression in the olfactory epithelium and olfactory bulb, I conducted *in situ* hybridization to multiple coronal sections spanning the entire olfactory turbinates and olfactory bulb in adult mice. In sections hybridized with antisense cRNA corresponding to the Cx57 coding sequence of 971-1339 (GenBank reference # NM_010289), notable hybridization signal was observed in the

sensory epithelium (Fig. 2). Hybridization signal was clearly weaker in tissues underneath the epithelium. Control experiments were conducted under the identical conditions with exception that antisense cRNA was replaced by the sense cRNA. Background signals were observed in sections hybridized with the sense cRNA (Fig. 2F).

The olfactory epithelium is a laminar pseudostratified epithelium comprising cell bodies that form the epithelium: sustentacular cells, olfactory neurons and basal cells. The apical one- to two- nucleus wide sublayer is largely made up by the cell bodies of sustentacular cells (Indicated by red arrows in Fig. 2A). On the other hand, basal cells are situated at the base of the epithelium adjacent to lamina propria. Somata of immature olfactory neurons may be found intermingled with, or slightly above, those of basal cells. The middle band of the epithelium, olfactory neuron sublayer, contains somata of mature olfactory neurons. Within the olfactory epithelium, hybridization signal was missing at the apical sublayer, suggesting that Cx57 transcript is not expressed in sustentacular cells. Hybridization signal was observed in the rest of the epithelial sublayers but abundance of the transcript varied from cells to cells. Fig. 2 provides a few examples of divergent distribution patterns of Cx57 positive cells within the olfactory epithelium. It was frequently observed that cells with strong hybridization staining were adjacent to those with faint or negative staining (Fig. 2A-2E). Intermingling of cells exhibiting varied abundance of the Cx57 transcript formed several patterns along the olfactory epithelium. However, distribution of these varied patterns did not appear to be associated with specific turbinates or olfactory receptor zones. Instead, varied patterns could be found in adjacent epithelium. As shown in Fig. 2D, cells having abundant hybridization signal distributed sparsely on the left side while cells at the center were largely unstained. Furthermore, a majority of the basal cells and olfactory neurons on the right had moderate hybridization staining. There were regions where the hybridization signal was stronger in the basal sublayer of the epithelium than that in the olfactory neuron sublayer (Fig. 2B) while opposite was true in other regions of the epithelium where the hybridization signal was missing in the basal sublayer but present in the olfactory neuron sublayer (Fig. 2C). In some areas of the epithelium the hybridization signal was scarce or missing in all three sublayers (Fig. 2D and 2E). When NIH ImageJ program was used to analysis RHI, the averaged RHI for the epithelium below the apical sustentacular cell sublayer ranged from 4.4 to 58.6 above that of the sustentacular cell sublayer measured in grayscales, further demonstrating the variability of Cx57 transcript expressed in the olfactory epithelium.

The olfactory bulb is the first relay station directly receiving input from the olfactory epithelium. A coronal section of the olfactory bulb shows layered organizations (Fig. 3A). The peripheral layer is the olfactory nerve layer, formed by bundles of olfactory axons before their entrance to the glomerular layer. The glomerular layer is formed by discrete glomeruli. Each glomerulus is filled with axon terminals of olfactory neurons expressing the same olfactory receptor, where they form synapses with dendrites of mitral cells and tufted cells, the principal neurons of the olfactory bulb, and with periglomerular cells surrounding the glomerulus. The tufted cells are large neurons scattered between the glomerular layer and the mitral cell layer. Tufted cells in the external plexiform layer are easy to spot based on their large sizes and cellular morphology. The mitral cell layer contains large mitral cells. In addition to receiving input from axons of olfactory neurons, mitral cells also synapse with granule cells, the interneurons placed in the central layer of the olfactory bulb. The thin internal plexiform layer separates the mitral cell layer from the granule cell layer.

In situ hybridization revealed that Cx57 positive cells were often arranged in patched distribution in the olfactory bulb as well. Hybridization positive cells were clustered in various locations including those in the accessory olfactory bulb. According to cellular morphology and locations, it was apparent that Cx57 positive cells included juxtaglomerular

cells (periglomerular cells and tufted cells) surrounding glomeruli, mitral cells in the mitral cell layer, and granule cells in the center of the olfactory bulb (Fig. 3A-3C). A few large Cx57 positive cells scattered around the external plexiform layer are tufted cells (pointed by arrowhead in Fig. 3A). The number of Cx57 positive juxtaglomerular cells surrounding a glomerulus varied. Many glomeruli did not have any Cx57 positive juxtaglomerular cells.

If we divide the olfactory bulb along the dorsal and ventral axes, the left half of the olfactory bulb as shown in Fig. 3A is the medial olfactory bulb and the right is the lateral olfactory bulb. In several coronal sections through the mid-rostral olfactory bulb, the hybridization signal was clearly stronger in the medial olfactory bulb compared to the lateral (Fig. 3A). More Cx57 positive cells were found in the medial side of the granule cell layer (M-GCL) and of the glomerular layer (M-GL) (comparison between left and right of two tilted black lines in Fig. 3A) while expression of Cx57 in the mitral cell layer was similar in either side of the bulb, indicating that divergent distribution of Cx57 positive cells in the medial and lateral olfactory bulbs is not caused by artifacts. In several sections, hybridization signal was weaker in dorsal regions of the olfactory bulb (Fig. 3A).

Data presented in Fig. 4 quantitatively demonstrate regional differences of Cx57 expression in the olfactory bulb. Quantitative analysis was conducted to sections in the mid-rostral olfactory bulb before the appearance of the accessory olfactory bulb. In these coronal sections of the olfactory bulb Cx57 hybridization staining in M-GCL, located at the left side of the two tilted black lines as shown in Fig. 3A, was compared to the corresponding right side of the lateral granule cell layer (L-GCL). M-GCL was 1.3±0.29 times as intensive as L-GCL on average in 22 bulbar sections examined ($p < 0.01$). Similarly, significant difference of Cx57 expression was observed in juxtaglomerular cells surrounding center medial glomerular layer (M-GL, areas indicated by the magenta line in Fig. 3A) compared to center lateral glomerular layer (L-GL, areas indicated by the green line in Fig. 3A) ($p < 0.001$, $n = 19$). In contrast, RHI between medial mitral cell layer (M-MCL) and lateral mitral cell layer (L-MCL) did not differ statistically ($p > 0.3$, $n = 19$). Comparison between dorsal-lateral glomerular layer (areas indicated by the cyan line in Fig. 3A) and the ventral-medial glomerular layer (areas indicated by the ruby red line in Fig. 3A) showed that the hybridization signal in the latter was twice as strong as the former on average. However, due to high variability among sections of the olfactory bulb, the difference between them was not statistically significant ($p > 0.1$, $n = 19$).

3. 2. Immunoreactivity of connexin 57

As described above, the anti-Cx57 antibody Ab40-5000MID recognized a single band at the expected molecular weight for Cx57 in homogenates of mouse olfactory turbinates (Fig. 1A). This antibody was used for immunohistochemistry to verify the presence of gap junction protein Cx57 in the olfactory epithelium and olfactory bulb. Using retina tissue as the positive control, immunoreactivity of Cx57 was observed in the olfactory epithelium and olfactory bulb (Fig. 5 and 6). Immunolabeling of the mouse retina showed similar patterns as described by Ciolofan et al. (2007) (Fig. 5A). Immunofluorescent puncta were found in the retinal outer plexiform layer. By comparison, immunointensity of Cx57 in the olfactory epithelium and olfactory bulb was weaker than that in the retinal outer plexiform layer. In both the olfactory epithelium and the olfactory bulb, immunoreactivity was largely detected in supranuclear cytoplasm of the cells. According to cellular morphology and their locations, these Cx57 immunoreactive cells are basal cells and olfactory neurons in the olfactory epithelium, and mitral cells, juxtaglomerular cells and granule cells in the olfactory bulb (Fig. 5C, 5D, and 6)

In both the olfactory epithelium and olfactory bulb, fewer cells were immunoreactive to Cx57 compared to the number of cells positive for *in situ* hybridization, a trend consistent

with expression of other connexin genes. Nevertheless, these immunoreactive cells in the olfactory epithelium and olfactory bulb were also arranged in patched patterns. Confocal images presented in Fig. 5C and 5D are examples of immunoreactivity of Cx57 in the olfactory epithelium. Fig 5C shows a region of the olfactory epithelium where immunoreactivity was observed in many cells. Immunolabeling was also observed in the apical sustentacular cell sublayer (pointed by arrows in Fig. 5C). It is probable that the staining was associated with dendrites of olfactory neurons. In many regions, none or only a few cells exhibited positive immunolabeling (Fig. 5D). Patched distribution of immunoreactive cells was also observed in the olfactory bulb. Large mitral cells had varied intensity of immunolabeling (Fig. 6A). Fig. 6B shows a glomerulus surrounded by several immunolabeled cells while in many other glomeruli, few or none of the surrounding juxtaglomerular cells were immunolabeled. Fig. 6C and 6D show two areas of the granule cell layer where the former has more Cx57 positive cells than the latter.

A recent study indicates that Cx57 forms dendro-dendritic and axo-axonal gap junctions in retinal horizontal cells and the immunolabeling is primary localized to the neuronal processes instead of somata (Janssen-Bienhold et al., 2009). However, it has been reported that immunolabeling of Cx57 is mainly localized to somata of neurons in regions of the cerebellum, brain stem and the spinal cord (Zappala' et al., 2010). Probably, varied cytoplasmic distributions of the Cx57 protein reflect different physiological states of cells. Since the overall immunolabeling of Cx57 in the olfactory epithelium and olfactory bulb was weaker than that in the retina, immunofluorescent puncta in the neuronal processes were often too weak to be distinguished from nonspecific background. For the same reason, it was difficult to use double immunolabeling methods to demonstrate whether expression of Cx57 was restricted to specific groups of neurons because the probability of nonspecific binding increases in double immunolabeling. In this study, I applied Sudan black to block autofluorescences before immunolabeling to eliminate influence of autofluorescences (Baschong et al., 2001; Viegas et al., 2007). This method reduced nonspecific fluorescences but sections treated with Sudan black were not suitable for double immunolabeling.

4. Discussion

This is the first anatomical and molecular biological report on distribution and expression of Cx57 in the olfactory system. The data show that within olfactory turbinates, Cx57 transcript is mainly distributed in the olfactory epithelial layer. With the exception of sustentacular cells, the Cx57 transcript is found in basal cells, mature and immature neurons in the olfactory epithelium. In the olfactory bulb, expression of Cx57 was observed in mitral cells, tufted cells, granule cells and periglomerular cells. A common feature for Cx57 expression in the olfactory epithelium and olfactory bulb is that Cx57 positive cells are sparsely distributed and often form small clusters. Scattered distribution of Cx57 positive cells in the olfactory epithelium and olfactory bulb correlates with the observation in the retina where expression of Cx57 was demonstrated by a gene targeting approach in which the Cx57 coding region was replaced by a LacZ reporter gene (Hombach et al., 2004). According to their study using Northern blot analysis, expression of Cx57 mRNA was detected in retina and thymus in a total of 14 tissues examined. These tissue samples included brain but did not include the olfactory system. However, expression of the Cx57 transcript in other regions of the nervous system has been demonstrated recently. Using both *in situ* hybridization and immunohistochemistry methods, Zappala' et al. (2010) have shown that Cx57 is expressed in the inferior olive, lateral reticular nucleus and motor trigeminal nucleus in the brain stem, in the Purkinje cells and cerebellar nuclei in the cerebellum, and in α-motoneurons in the spinal cord. In this study, I have provided evidence that Cx57 mRNA is expressed in a variety of neurons in the olfactory epithelium and olfactory bulb. The immunointensity of Cx57 in the olfactory system was weaker than that found in the retinal

outer plexiform layer. Weak immunolabeling of Cx57 in the olfactory system prohibits further investigation on its association with specific groups of cells using additional protein markers since the probability of nonspecific binding increases in double immunolabeling.

Demonstration of Cx57 expression in the olfactory system has expanded our knowledge on tissue distributions of Cx57. Cytoplasmic immunolabeling of Cx57 was observed in neurons in the olfactory epithelium and olfactory bulb. Cytoplasmic localization of the Cx57 protein was also reported in neurons in the brain stem, cerebellum, and the spinal cord (Zappala' et al., 2010). However, immunofluorescent puncta of Cx57 is largely distributed in neuronal processes in the horizontal cells of retina to form dendro-dendritic and axo-axonal gap junctions while their somata are depleted of immunoreactivity (Janssen-Bienhold et al., 2009). These studies indicate that under different conditions, subcellular distribution of the Cx57 protein may vary. This concept correlates with the findings in other connexin proteins. Ample data have shown that at different stages of its life cycle the Cx43 protein is localized to distinct subcellular regions. (Lauf et al., 2002; Dbouk et al., 2009; Solan and Lampe, 2009).

Expression of connexins is activity dependent. A reduction in Cx57 expression was observed in dark adapted retina (Kihara et al., 2006). Light exposure changes distribution of Cx57 immunoreactivity in the mouse retina (Janssen-Bienhold et al., 2009). Increased expression of Cx57 in the cerebellum was observed in drug-induced somatic tremor (Zappala' et al., 2010). Although it is unknown how olfactory activity may modulate Cx57 expression in the olfactory system at the present, activity dependent changes of Cx43 expression were observed in the olfactory epithelium (Zhang et al., 2007). Activity dependent modulation of connexins constitutes a probable ground for a common theme on expression of connexins in that, almost in all cases, the number of cells expressing mRNA is significantly higher than the number of immunoreactive cells, which means that in some cells although the connexin transcript is expressed the protein level is too low to be detected by immunohistochemistry methods. Presence of connexin mRNA creates a basis for cells to synthesize proteins in a speedy fashion when gap junction proteins are required under certain physiological conditions. A short half-life also contributes low concentrations of connexin proteins in cells, which further stresses importance of connexins in dynamic regulation of physiological functions. Accumulating data have demonstrated that connexins play a broader role than we would envision decades ago, including their involvement in maintaining homeostasis, regulating cell proliferation and differentiation, and apoptosis (Trosko, 2007; Kardami et al., 2007; Vinken et al., 2009). Connexin family is a group of genes whose expression was tightly modulated from transcription to posttranslation. For example, promoters of Cx43 contain multiple regulatory binding sites. Three promoters are responsible for production of nine different Cx43 transcripts within a cell (Yu et al., 1994; Pfeifer et al., 2004). Furthermore, its protein translation is negatively regulated by the MiR-200 family of microRNA (Rash et al., 2005; Anderson et al., 2006). The olfactory epithelium expresses a repertoire of over 100 microRNAs, while members of the MiR-200 family play key roles in differentiation and neurogenesis (Choi et al., 2008). How microRNA regulates connexin protein levels and consequently influences biological processes is a subject for future study. Demonstration of Cx57 expression in the olfactory system allows us to take consideration of involvement of Cx57 in a variety of biological functions in coming studies.

The protein level of Cx57 in the olfactory epithelium and olfactory bulb is lower than that observed in the retina. Similar conclusion can be drawn from expression of Cx36. Although the Cx36 protein level is relatively high in glomeruli located at the rostral olfactory bulb and near the accessory olfactory bulb (Zhang and Restrepo, 2003), its overall expression is lower than that in the retina (unpublished results). Maintaining low levels of connexin expression

may be typical for a heterogeneous system such as the olfactory epithelium and olfactory bulb since low densities of gap junctions could be a result of selective coupling between cells in a complex system. Furthermore, different strengths of coupling between cells lead to different physiological consequences. A low degree of coupling is beneficial in reducing systemic noise (Buntinas et al., 2005) while moderate to high levels of coupling, as shown in the visual system, may be more suitable to increase signal strength.

Connexin 57 is important for visual acuity. In their studies on Cx57 knock out mice, Shelley et al. (2006) showed that deletion of Cx57 led to a reduction of horizontal cell receptive field accompanying with decreased cellular responses to light stimuli. Expression of the Cx57 protein in the retina is regulated by light stimuli (Kihara et al., 2006; Janssen-Bienhold et al., 2009). Whether and how Cx57 influences olfactory sensitivity has yet to be explored. Evidence shows that functional disruption of gap junctions in olfactory neurons reduces olfactory sensitivity (Zhang, 2010). In the olfactory bulb, Cx36 mediated gap junction coupling contributes to mitral cell lateral excitation (Christie and Westbrook, 2006). Electronic coupling among mitral cells is an important mechanism to ensure temporally coherent output from an odor-specific glomerular unit (Schoppa and Westbrook, 2002; Christie et al., 2005). Gap junctions may contribute to slow membrane oscillations among external tufted cells (Hayar et al., 2005). Presence of gap junctions in the periglomerular cells, mitral cells and granule cells has been demonstrated by ultrastructural studies (Reyher et al., 1991, Kosaka and Kosaka, 2003, 2004, 2005). Some of these gap junctions are made by Cx36 or Cx45 (Kosaka et al., 2005; Rash et al., 2005). Our previous and current studies suggest that a variety of connexins, including Cx57, is expressed in neurons in the olfactory epithelium and olfactory bulb. These anatomical data have provided a solid basis for research on how different connexins play distinct roles in olfactory transduction in the future.

Acknowledgments

The author thanks the anonymous reviewers for their constructive suggestions. The work was supported by NIH grant DC04952 and startup funds from the Illinois Institute of Technology.

References

Anderson C, Catoe H, Werner R. MIR-206 regulates connexin43 expression during skeletal muscle development. Nucleic Acids Res. 2006; 34:5863–5871. [PubMed: 17062625]

Baschong W, Suetterlin R, Laeng RH. Control of autofluorescence of archival formaldehyde-fixed, paraffin-embedded tissue in confocal laser scanning microscopy (CLSM). J Histochem Cytochem. 2001; 49:1565–1572. [PubMed: 11724904]

Buntinas L, Zhang C, Restrepo D. Biophysical model of olfactory receptor neuron pairs reveals mechanism for gap junction mediated synchronized firing at threshold odor concentrations. Chem Senses. 2005; 30:A83–A84.

Choi PS, Zakhary L, Choi WY, Caron S, varez-Saavedra E, Miska EA, McManus M, Harfe B, Giraldez AJ, Horvitz HR, Schier AF, Dulac C. Members of the miRNA-200 family regulate olfactory neurogenesis. Neuron. 2008; 57:41–55. [PubMed: 18184563]

Christie JM, Bark C, Hormuzdi SG, Helbig I, Monyer H, Westbrook GL. Connexin36 mediates spike synchrony in olfactory bulb glomeruli. Neuron. 2005; 46:761–772. [PubMed: 15924862]

Christie JM, Westbrook GL. Lateral excitation within the olfactory bulb. J Neurosci. 2006; 26:2269–2277. [PubMed: 16495454]

Ciolofan C, Lynn BD, Wellershaus K, Willecke K, Nagy JI. Spatial relationships of connexin36, connexin57 and zonula occludens-1 in the outer plexiform layer of mouse retina. Neuroscience. 2007; 148:473–488. [PubMed: 17681699]

Dbouk HA, Mroue RM, El-Sabban ME, Talhouk RS. Connexins: a myriad of functions extending beyond assembly of gap junction channels. Cell Commun Signal. 2009; 7:4. [PubMed: 19284610]

Hayar A, Shipley MT, Ennis M. Olfactory bulb external tufted cells are synchronized by multiple intraglomerular mechanisms. J Neurosci. 2005; 25:8197–8208. [PubMed: 16148227]

Hombach S, Janssen-Bienhold U, Sohl G, Schubert T, Bussow H, Ott T, Weiler R, Willecke K. Functional expression of connexin57 in horizontal cells of the mouse retina. Eur J Neurosci. 2004; 19:2633–2640. [PubMed: 15147297]

Janssen-Bienhold U, Trumpler J, Hilgen G, Schultz K, Muller LP, Sonntag S, Dedek K, Dirks P, Willecke K, Weiler R. Connexin57 is expressed in dendro-dendritic and axo-axonal gap junctions of mouse horizontal cells and its distribution is modulated by light. J Comp Neurol. 2009; 513:363–374. [PubMed: 19177557]

Kardami E, Dang X, Iacobas DA, Nickel BE, Jeyaraman M, Srisakuldee W, Makazan J, Tanguy S, Spray DC. The role of connexins in controlling cell growth and gene expression. Prog Biophys Mol Biol. 2007; 94:245–264. [PubMed: 17462721]

Kihara AH, de Castro LM, Moriscot AS, Hamassaki DE. Prolonged dark adaptation changes connexin expression in the mouse retina. J Neurosci Res. 2006; 83:1331–1341. [PubMed: 16496335]

Koling A, Sandmark B, Rask-Andersen H, Deuschl H. Gap junctions in the human olfactory mucosa as demonstrated by freeze-fracture electron microscopy. Cell Biol Int Rep. 1988; 12:563. [PubMed: 3180238]

Kosaka T, Deans MR, Paul DL, Kosaka K. Neuronal gap junctions in the mouse main olfactory bulb: morphological analyses on transgenic mice. Neuroscience. 2005; 134:757–769. [PubMed: 15979807]

Kosaka T, Kosaka K. Neuronal gap junctions in the rat main olfactory bulb, with special reference to intraglomerular gap junctions. Neurosci Res. 2003; 45:189–209. [PubMed: 12573466]

Kosaka T, Kosaka K. Neuronal gap junctions between intraglomerular mitral/tufted cell dendrites in the mouse main olfactory bulb. Neurosci Res. 2004; 49:373–378. [PubMed: 15236862]

Kosaka T, Kosaka K. Intraglomerular dendritic link connected by gap junctions and chemical synapses in the mouse main olfactory bulb: electron microscopic serial section analyses. Neuroscience. 2005; 131:611–625. [PubMed: 15730867]

Kreuzberg MM, Deuchars J, Weiss E, Schober A, Sonntag S, Wellershaus K, Draguhn A, Willecke K. Expression of connexin30.2 in interneurons of the central nervous system in the mouse. Mol Cell Neurosci. 2008; 37:119–134. [PubMed: 17942321]

Lauf U, Giepmans BN, Lopez P, Braconnot S, Chen SC, Falk MM. Dynamic trafficking and delivery of connexons to the plasma membrane and accretion to gap junctions in living cells. Proc Natl Acad Sci U S A. 2002; 99:10446–10451. [PubMed: 12149451]

Miragall F, Hwang TK, Traub O, Hertzberg EL, Dermietzel R. Expression of connexins in the developing olfactory system of the mouse. J Comp Neurol. 1992; 325:359–378. [PubMed: 1332989]

Miragall F, Simburger E, Dermietzel R. Mitral and tufted cells of the mouse olfactory bulb possess gap junctions and express connexin43 mRNA. Neurosci Lett. 1996; 216:199–202. [PubMed: 8897492]

Pereda A, O'Brien J, Nagy JI, Smith M, Bukauskas F, Davidson KG, Kamasawa N, Yasumura T, Rash JE. Short-range functional interaction between connexin35 and neighboring chemical synapses. Cell Commun Adhes. 2003; 10:419–423. [PubMed: 14681051]

Pfeifer I, Anderson C, Werner R, Oltra E. Redefining the structure of the mouse connexin43 gene: selective promoter usage and alternative splicing mechanisms yield transcripts with different translational efficiencies. Nucleic Acids Res. 2004; 32:4550–4562. [PubMed: 15328367]

Rash JE, Davidson KG, Kamasawa N, Yasumura T, Kamasawa M, Zhang C, Michaels R, Restrepo D, Ottersen OP, Olson CO, Nagy JI. Ultrastructural localization of connexins (Cx36, Cx43, Cx45), glutamate receptors and aquaporin-4 in rodent olfactory mucosa, olfactory nerve and olfactory bulb. J Neurocytol. 2005; 34:307–341. [PubMed: 16841170]

Rash JE, Yasumura T, Davidson KG, Furman CS, Dudek FE, Nagy JI. Identification of cells expressing Cx43, Cx30, Cx26, Cx32 and Cx36 in gap junctions of rat brain and spinal cord. Cell Commun Adhes. 2001; 8:315–320. [PubMed: 12064610]

Reyher CK, Lubke J, Larsen WJ, Hendrix GM, Shipley MT, Baumgarten HG. Olfactory bulb granule cell aggregates: morphological evidence for interperikaryal electrotonic coupling via gap junctions. J Neurosci. 1991; 11:1485–1495. [PubMed: 1904478]

Schoppa NE, Westbrook GL. AMPA autoreceptors drive correlated spiking in olfactory bulb glomeruli. Nat Neurosci. 2002; 5:1194–1202. [PubMed: 12379859]

Shelley J, Dedek K, Schubert T, Feigenspan A, Schultz K, Hombach S, Willecke K, Weiler R. Horizontal cell receptive fields are reduced in connexin57-deficient mice. Eur J Neurosci. 2006; 23:3176–3186. [PubMed: 16820008]

Solan JL, Lampe PD. Connexin43 phosphorylation: structural changes and biological effects. Biochem J. 2009; 419:261–272. [PubMed: 19309313]

Trosko JE. Gap junctional intercellular communication as a biological "Rosetta stone" in understanding, in a systems biological manner, stem cell behavior, mechanisms of epigenetic toxicology, chemoprevention and chemotherapy. J Membr Biol. 2007; 218:93–100. [PubMed: 17960321]

Viegas MS, Martins TC, Seco F, do Carmo A. An improved and cost-effective methodology for the reduction of autofluorescence in direct immunofluorescence studies on formalin-fixed paraffin-embedded tissues. Eur J Histochem. 2007; 51:59–66. [PubMed: 17548270]

Vinken M, De RE, Decrock E, De VE, Leybaert L, Vanhaecke T, Rogiers V. Epigenetic regulation of gap junctional intercellular communication: more than a way to keep cells quiet? Biochim Biophys Acta. 2009; 1795:53–61. [PubMed: 18801412]

Yu W, Dahl G, Werner R. The connexin43 gene is responsive to oestrogen. Proc Biol Sci. 1994; 255:125–132. [PubMed: 8165225]

Zappala' A, Parenti R, La Della F, Cicirata V, Cicirata F. Expression of connexin57 in mouse development and in harmaline-tremor model. Neuroscience. 2010

Zhang C. Gap junctions in olfactory neurons modulate olfactory sensitivity. BMC Neurosci. 2010; 11:108. [PubMed: 20796318]

Zhang C, Finger TE, Restrepo D. Activity-dependent regulation of connexin expression in the olfactory epithelium. Chem Senses. 2007; 32:A70.

Zhang C, Finger TE, Restrepo D. Mature olfactory receptor neurons express connexin 43. J Comp Neurol. 2000; 426:1–12. [PubMed: 10980480]

Zhang C, Restrepo D. Understanding the role of gap junctions in olfactory function. Chem Senses. 2005; 30:A1.

Zhang C, Restrepo D. Expression of connexin 45 in the olfactory system. Brain Res. 2002; 929:37–47. [PubMed: 11852029]

Zhang C, Restrepo D. Heterogeneous expression of connexin 36 in the olfactory epithelium and glomerular layer of the olfactory bulb. J Comp Neurol. 2003; 459:426–439. [PubMed: 12687708]

Research Highlights

- Expression of Cx57 in the olfactory epithelium is demonstrated using three research approaches.
- In the olfactory epithelium, basal cells and olfactory neurons express Cx57.
- Cx57 is expressed in juxtaglomerular cells, mitral cells and granule cells in the olfactory bulb.
- Patterned distributions of Cx57 positive cells are described.
- Immunoreactivity of Cx57 is weaker in the olfactory system compared to the retina.

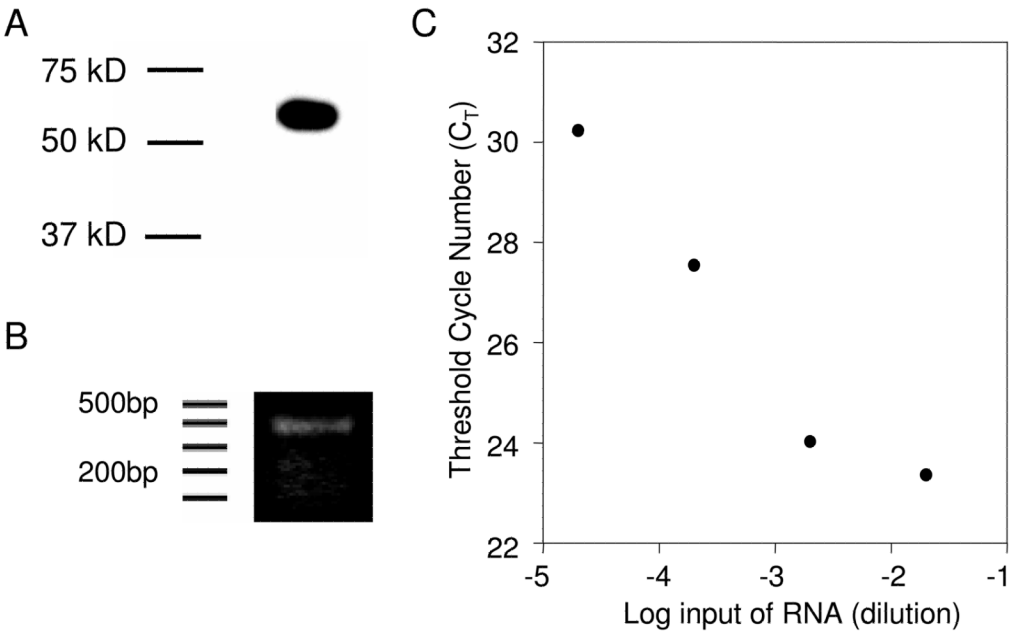

Fig. 1.

Expression of Cx57 in the olfactory epithelium. (A) Western blot analysis of homogenates of adult olfactory turbinates revealed a single band between 50 and 75 kDa when the rabbit anti-Cx57 antibody (Ab40-5000MID) was used. (B) Reverse transcription of PCR reaction using total RNA from olfactory turbinates generated a fragment of Cx57 cDNA. (C) A negative logarithmic linear relationship of the Cx57 DNA product between the amounts of total RNA added and the threshold cycle number C_T in a real time quantitative PCR reaction.

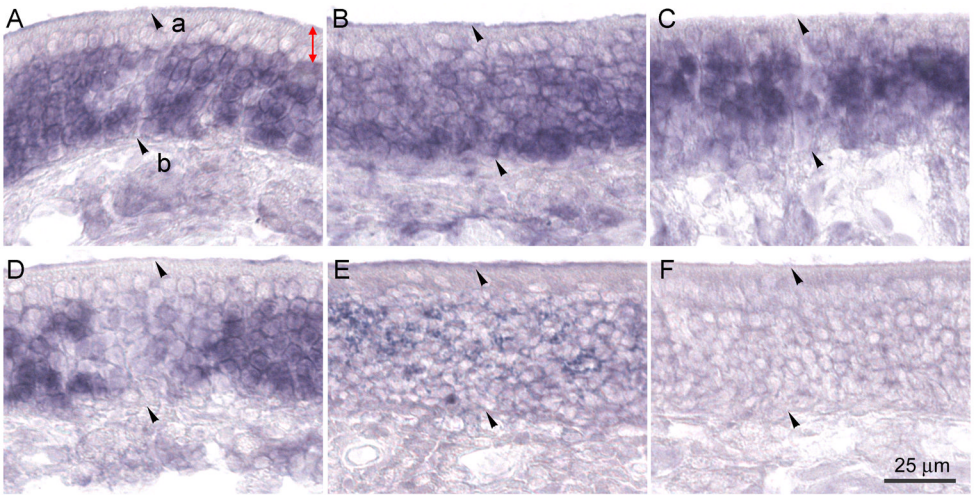

Fig. 2.

Distribution patterns of cells expressing the Cx57 transcript in the olfactory epithelium. (A) to (E) are photomicrographs obtained from different regions of the olfactory epithelium when antisense Cx57 cRNA was used as the probe for *in situ* hybridization. (F) A photomicrograph from the olfactory epithelium when the sense Cx57 cRNA was used as the probe (control). The apical surface (a) of the epithelium and the basal lamina (b) are pointed by arrowheads showing the range of the epithelial layer. Red arrows shown in (A) indicate the approximate depth of sustentacular cell sublayer.

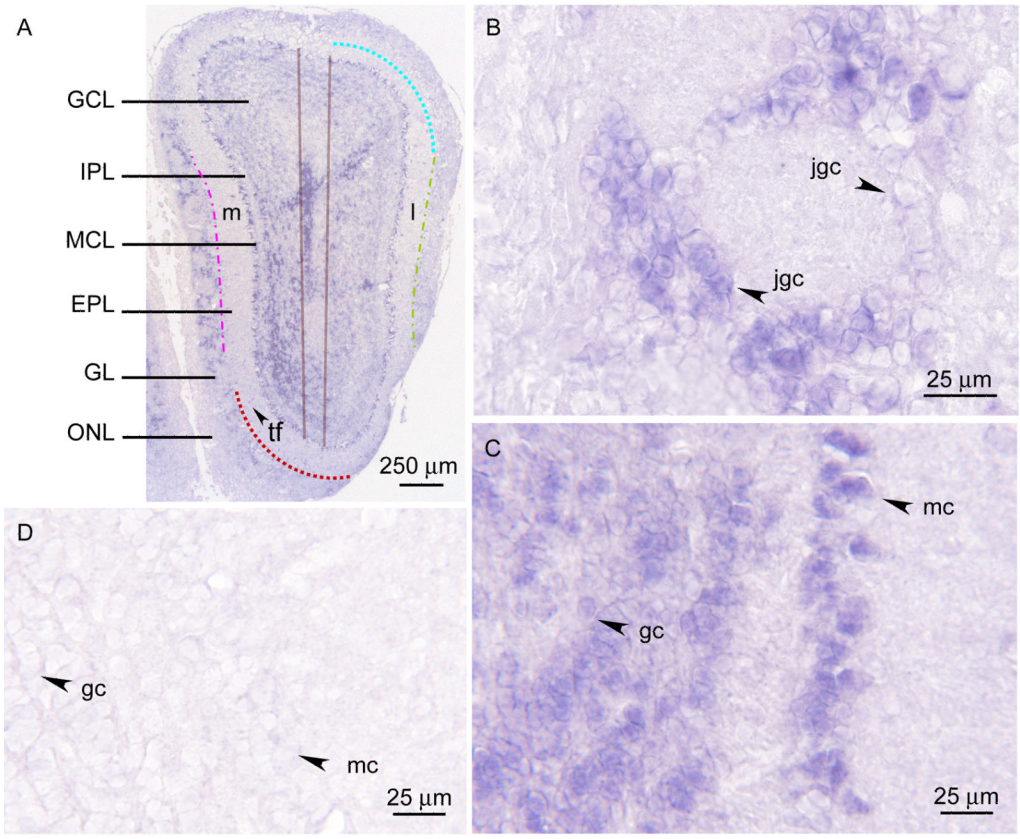

Fig. 3.

Expression of the Cx57 transcript in the olfactory bulb. (A) Low magnification photomicrograph of a coronal section of the olfactory bulb. The olfactory bulb shows layered structures. From the periphery to center are the olfactory nerve layer (ONL), glomerular layer (GL), external plexiform layer (EPL), mitral cell layer (MCL), internal plexiform layer (IPL) and the granule cell layer (GCL). The medial side of the olfactory bulb is marked by “m” and the lateral side by “l”. Color coded lines indicate the areas for quantitative analysis as described in the text. The arrowhead points to a few tufted cells (tf). (B) High magnification of the photomicrograph showing a glomerulus surrounded by juxtaglomerular cells (jgc) that are positive or negative for Cx57 expression. (C) and (D) are regions containing granule cells (gc) and mitral cells (mc) in the sections hybridized with the antisense Cx57 cRNA probe (C) or sense Cx57 cRNA probe (D).

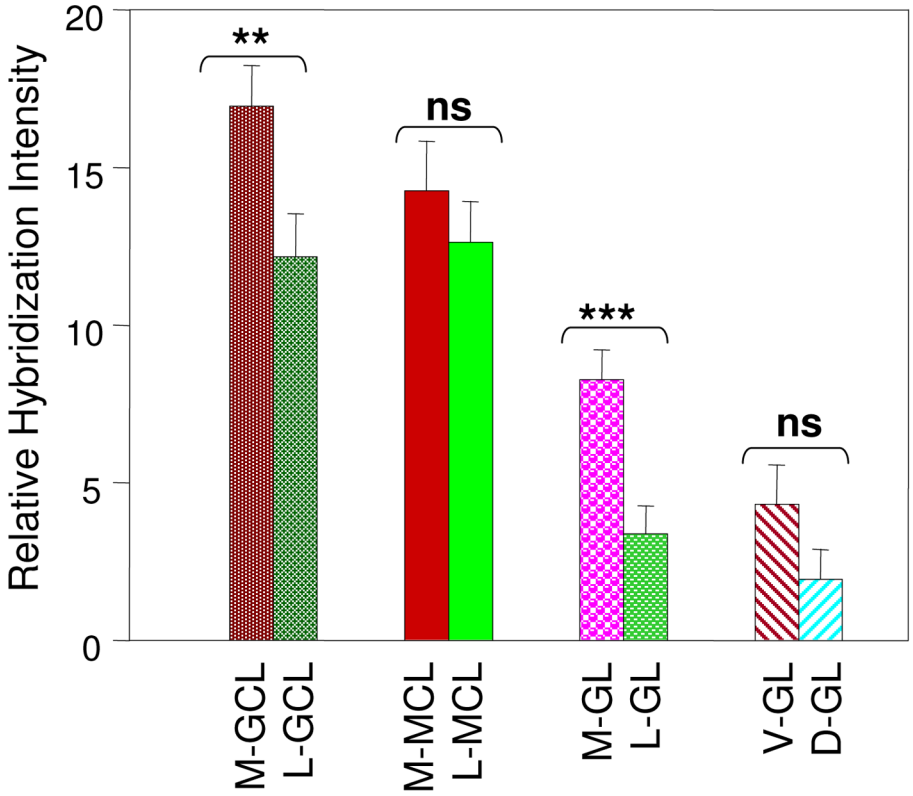

Fig. 4.

Regional differences of Cx57 expression in the olfactory bulb. The bar graph shows averaged Relative Hybridization Intensity in the medial granule cell layer (M-GCL), lateral granule cell layer (L-GCL), medial mitral cell layer (M-MCL), lateral mitral cell layer (L-MCL), medial glomerular layer (M-GL), lateral glomerular layer (L-GL), ventral glomerular layer (V-GL) and dorsal glomerular Layer (D-GL). The regions included for quantitative measurements are indicated in Fig. 3A and described in the text. Paired t-test was used for statistical analysis. ns, not different statistically; **, $p < 0.01$; ***, $p < 0.001$.

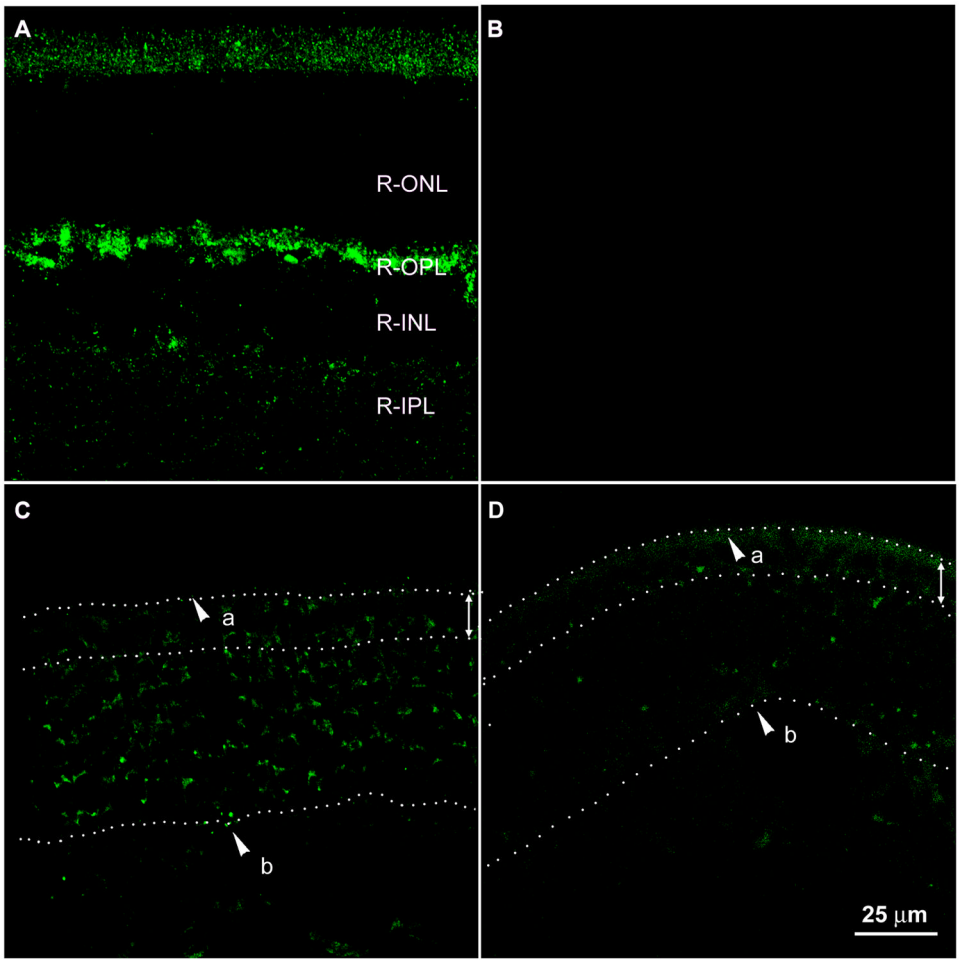

Fig. 5.

Comparison of immunointensity of Cx57 between the retina and the olfactory epithelium. (A) and (B) Confocal scanning of the retina that was immunolabled by a antibody against Cx57 (A) and the negative control that was processed under the same condition without presence of the Cx57 antibody (B). Layers of the retina are indicated by abbreviations: the retinal outer nuclear layer (R-ONL), retinal outer plexiform layer (R-OPL), retinal inner nuclear layer (R-INL), and the retinal inner plexiform layer (R-IPL). (C) and (D) are images of the olfactory epithelium showing varied degrees of immunoreactivity in different regions of the epithelium. Arrowheads point to the apical surface (a) and basal lamina (b) of the olfactory epithelium. In addition, positions of the apical surface and basal lamina were outlined by the dotted lines. The second dotted line below the apical surface highlights approximate locations of the sustentacular cell sublayer (marked by white arrows). The negative control of the olfactory epithelium (not shown) did not exhibit immunoreactivity.

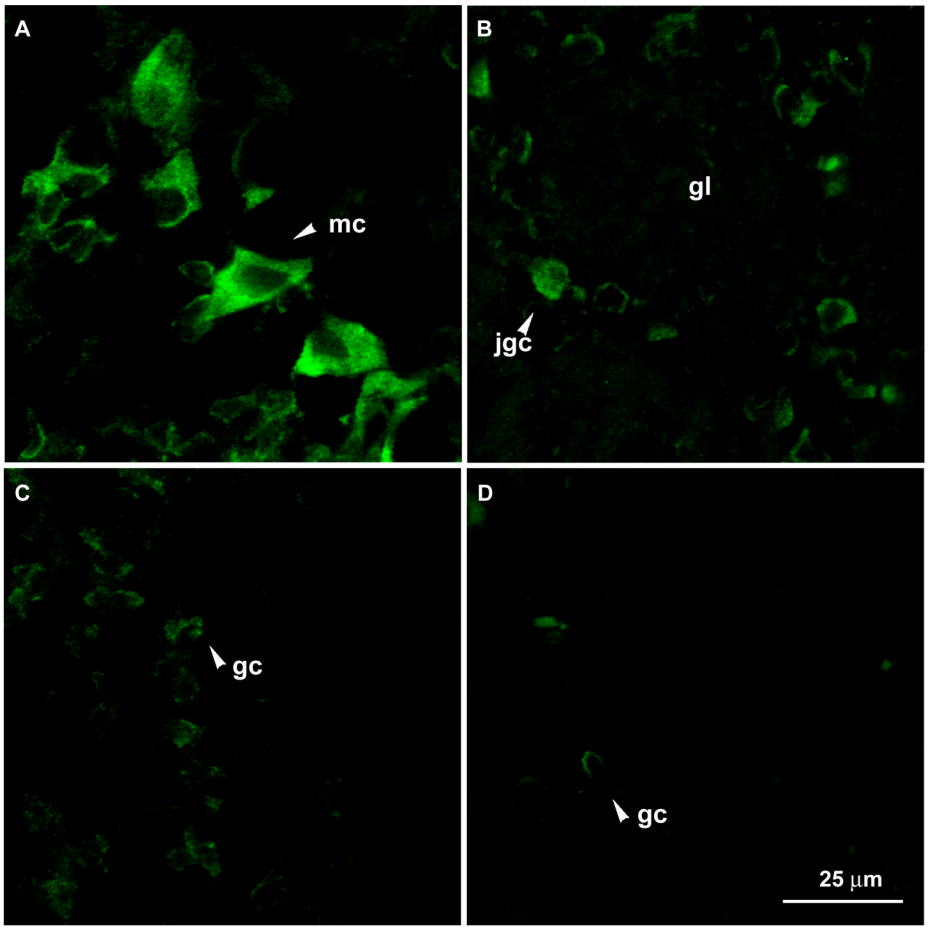

Fig. 6.

Immunoreactivity of Cx57 in neurons in the olfactory bulb. Confocal images from the olfactory bulb show immunolabeling of Cx57 in mitral cells (mc) (A), in juxtaglomerular cells (jgc) surrounding a glomerulus (gl) (B), and in granule cells (gc) (C and D). All images were processed under the identical conditions. The negative control of the olfactory bulb (not shown) did not exhibit immunoreactivity.